

## NUMERICAL ASSESSMENT OF WIND-DRIVEN RAIN CATCH RATIO

### Marc O. Abadie

Visiting researcher at Thermal Systems Laboratory - LST  
Pontifical Catholic University of Parana – PUCPR/CCET  
Rua Imaculada Conceição, 1155  
Curitiba – PR – 80215-901 – Brazil  
mabadie@univ-lr.fr

### Nathan Mendes

Thermal Systems Laboratory - LST  
Pontifical Catholic University of Parana – PUCPR/CCET  
Rua Imaculada Conceição, 1155  
Curitiba – PR – 80215-901 – Brazil  
nathan.mendes@pucpr.br

**Abstract.** *The present study aims to evaluate the importance of taking into account the wind turbulence when performing droplet trajectory numerical simulations. The turbulence effect on Wind-Driven Rain is studied by calculating the specific catch ratio of 1mm droplets for an isolated low-rise building windward surface under a 5m/s normal wind. An Eulerian Second Moment Closure and a Lagrangian one-way coupling models are used to calculate the airflow field and the droplet trajectories respectively. Results show that turbulence has a negligible effect in the case of the building whole windward wall but can substantially modify the value of the specific catch ratio in the case of Wind-Driven Rain gauges.*

**Keywords.** *Wind-Driven Rain, Specific Catch Ratio, Turbulence Intensity, Reynolds Stress Model.*

### 1. Introduction

Moisture-associated problems have become an important subject of research in the building physics area. Indoor humidity is an essential parameter to determine the occupants' perception of indoor air quality, and is also an important cause of harmful processes that may occur on surfaces of buildings, such as material deterioration and microbial growth. The on-going research program of the International Energy Agency (2006) even aims to evaluate its importance on the building heating and cooling energy loads. New generation of Building Energy Simulation tools such as WUFI (1994), WUFI-Bio (2001), PowerDomus (2003) already integrates both heat and moisture calculations including capillary migration, and can be employed to evaluate the coupled effect of heat and moisture (vapour and liquid) transfer through building envelopes. The specification of boundary conditions, and more particularly outdoor ones, is of great importance in order to obtain reliable results.

As Wind-Driven Rain (WDR) is one of the most important moisture sources affecting building envelopes, important research efforts have been conducted in the last twenty years. The main goal of those studies lies in the evaluation of one parameter, the so-called catch ratio, that links the unobstructed horizontal rainfall intensity to the WDR intensity on the building. The catch ratio that integrates the whole spectrum of droplet sizes is deduced from the specific catch ratio, that is related to only one droplet size, and the rainfall intensity by the relation of Best (1950). The catch ratio thus depends on several parameters: the building geometry (including the surroundings), the position on the building façade, the reference wind velocity, the horizontal rainfall intensity and horizontal raindrop-size distribution.

This WDR catch ratio can be evaluated by both on-site measurements and numerical simulations. Recently, Blocken and Carmeliet (2004) have provided a literature review of Computational Fluid Dynamics (CFD) studies and, by comparing their numerical results to experimental measurements, have concluded that CFD modelling can accurately predict WDR catch ratios. The mean error on the catch ratio values for the studied windward wall was 0.03 equivalent to a 8% relative error and, contrary to the simulations, rain has been found on a leeward wall. According to the authors, these discrepancies can be explained either by the precision of the measurements and by the fact that the turbulence of the airflow was not modelled in their simulations. The first potential cause has been investigated by the same authors (2006) who demonstrated that the measurement actually depends on the type of gauge used to collect the rain droplets. On the other hand, the role the wind turbulence plays on the droplets trajectory and its importance on WDR investigation still remain a subject of controversy among researchers. Lakehal *et al.* (1995) found that droplets are too heavy for their trajectories to be really perturbed by turbulence, even close to the walls. Sankaran and Paterson (1995) concluded that turbulence is of great importance in the case of tall buildings. Choi (1997) showed that turbulence is negligible for droplets of 5mm and 2mm in diameter but modifies 1mm droplets specific catch ratio by 0.02 with stronger effect in the lower part of the façade. Hagan *et al.* (1999) found that large discrepancies between the

experiment and numerical results in the upper part of its higher buildings and in the middle zone of its lower one. The author attributed those differences to inaccurate modelling of the wind turbulence and, as a consequence, meant that turbulence needs to be correctly calculated to improve WDR analysis.

The present study aims to assess the importance of modelling turbulence on the numerical evaluation of the WDR specific catch ratio. Three-dimensional simulations are performed to estimate the specific catch ratio of 1 mm droplet on an isolated low-rise building. After the description of the computational domain, the motivations of the choice of the turbulence model are presented and the obtained airflow field is compared to the available literature results. In a second part, the lagrangian model used to calculate the droplet trajectories within the domain is described. Specific catch ratios are evaluated with and without turbulence effects and are calculated for the whole windward surface and for prototypical gauges located at different positions of the same surface.

## 2. Simulation of the airflow around an isolated low-rise building

Figure (1) presents the studied domain which is basically made up of a cylinder (diameter: 35m, height: 10m) and a parallelepipedic building located at its centre. External dimensions of the building were chosen according to the BESTEST model. This physical model was used in a large range of case studies concerning building energy simulation validation (Judkoff and Neymark, 1995). Note that the two windows of the south wall are not included in the present simulation. In each simulation, four contiguous octants have been used as inlets while the four others as outlets to allow simulating eight different wind directions. The cylinder radius has been calculated according to the critical Reynolds expression in order to obtain a fully-turbulent boundary layer at the building's location. A power-law expression has been considered to represent the velocity profile at the boundary conditions according to the one that has been used by Davenport (1960). In the present analysis, the reference wind speed has been set to 5m/s and the wind remains normal to the longest side of the building. It has also been assumed that there is a temperature difference of 10°C between the building surfaces and the surrounding air.

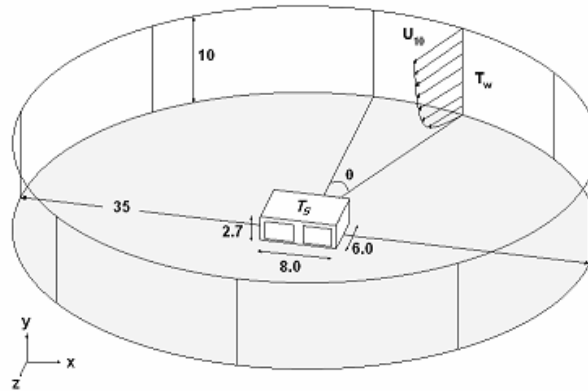


Figure 1. Domain geometry (dimensions are in meter).

The predictions are performed by the analysis of a three-dimensional steady-state incompressible flow based on the Reynolds-average approach. The governing equations for the conservation of mass, momentum and energy are:

$$\frac{\partial \bar{u}_i}{\partial x_i} = 0 \quad (1)$$

$$\frac{\partial (\bar{u}_j \bar{u}_i)}{\partial x_j} = -\frac{\partial \bar{P}}{\partial x_i} + \nu \nabla^2 \bar{u}_i + \frac{\partial}{\partial x_j} (-\overline{u_i' u_j'}) + \rho g_i \beta (T_{ref} - T) \quad (2)$$

$$\frac{\partial (\bar{u}_j T)}{\partial x_j} = \alpha \nabla^2 T + \frac{\partial}{\partial x_j} (-\overline{u_j' t'}) \quad (3)$$

where  $\bar{u}_i$  is the  $i^{\text{th}}$  component of the air mean velocity (m/s),  $x_i$  is the  $i^{\text{th}}$  component of the coordinate system (m),  $\bar{P}$  is the air mean absolute pressure (Pa),  $\nu$  is the molecular kinematic viscosity ( $\text{m}^2/\text{s}$ ),  $u_i'$  is the  $i^{\text{th}}$  component of the air fluctuating velocity (m/s),  $\rho$  is the air density ( $\text{kg}/\text{m}^3$ ),  $g_i$  is the  $i^{\text{th}}$  component of the gravitational acceleration ( $\text{m}/\text{s}^2$ ),  $\beta$  is the air thermal expansion coefficient ( $1/\text{K}$ ),  $T_{ref}$  is the reference air mean temperature (K),  $T$  is the air mean

temperature (K),  $\alpha$  is the air thermal diffusivity ( $m^2/s$ ) and  $t'$  is the air fluctuating temperature (K). The unknowns,  $\overline{u_i' u_j'}$  and  $\overline{u_j' t'}$ , constitute the second-moment statistical correlation or so-called Reynolds stresses and turbulent heat fluxes.

The crucial choice of the turbulence model depends on the problem to be solved. Previous researchers on Wind-Driven Rain have employed the most commonly used models in engineering, *e.g.*, eddy viscosity models such as standard  $k-\epsilon$  model for Lakehal *et al.* (1995), Van Mooke *et al.* (1997), Karagiozis *et al.* (1997), Choi (1997 and 1999) and Hagan (1999) or Realizable  $k-\epsilon$  model for Blocken and Carmeliet (2002 and 2006) despite their well-known problems such as the turbulent kinetic energy overproduction in stagnant regions (that is attenuated by the Realizable  $k-\epsilon$  model) and the assumption of isotropy of the normal Reynolds stresses. In the case of Wind-Driven Rain simulation, two important issues need to be taken into consideration. First, the presence of the ground and building envelope induces a strong anisotropy on the Reynolds stresses. Second, the current problem presents a highly complex separated flow around the building. By investigating the behaviour of WDR in 2D urban canopy, Lakehal *et al.* (1995) have concluded that the use of Second Moment Closure model is more appropriated than standard  $k-\epsilon$  model. Compared to eddy-viscosity models which will not perform well in this case, Reynolds stresses (or Second Moment Closure) model (RSM) is expected to give improvements on both aspects as it naturally includes the effects of streamline curvature, sudden changes in the strain rate, secondary flows and buoyancy by solving differential transport equations individually for each Reynolds stress component.

As shown by Meroney *et al.* (1999) and Fothergill *et al.* (2002), results obtained with RSM for flows around obstacles are often better than with eddy viscosity models but their main deficiencies lie in the simulation of boundary layers which comes from the underlying  $\epsilon$ -equation. Particularly the accurate prediction of flow separation, like in the present case, is problematic when the  $\epsilon$ -equation is used. The use of the  $\omega$ -equation instead of the  $\epsilon$ -equation avoid those issues. The turbulent model used in the present study is the Baseline (BSL) Reynolds Stress Model (CFX, 2004), which is identical to the RSM  $\omega$ -equation based model for the inner region of a boundary and gradually changes to the standard RSM  $\epsilon$ -equation based model in the outer wake region by the mean of a blending function. This coupling formulation permits to avoid strong sensitivity to free stream conditions implied by the  $\omega$ -equation based formulation (Menter, 1993). Reynolds stress transport equations, pressure-strain correlation and coefficient values employed in the present study can be found in CFX (2004).

A commercial CFD program (CFX, 2004) has been used for numerical prediction of the airflow. The governing equations have been solved with a segregated scheme and a first-order upwind advection scheme has been adopted. The continuity equation is a second-order central difference approximation to the first-order derivative in velocity, modified by a fourth derivative in pressure which acts to redistribute the influence of the pressure. The local criterion for numerical convergence, *i.e.*, root mean square residuals between two consecutive iterations, is lower than  $10^{-4}$ .

A three-dimensional unstructured grid of 774,000 cells has been generated to solve the present problem. The quality of this grid has been verified and improved performing iterative simulations for each configuration in order to obtain a  $y^+$  value between 20 and 100.

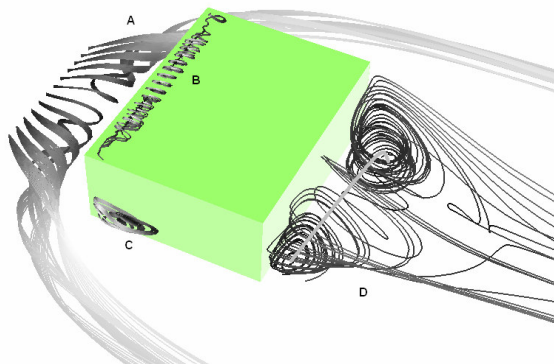


Figure 2. Streamlines showing the airflow vortices.

Figure (2) presents the main features of the three-dimension airflow field in the case of a South wind. The horseshoe vortex (A), the roof vortex (B), the two lateral side vortices (C) and the arch vortex (D) in the re-attachment region behind the building are all well predicted in the present simulation. Turbulent structures around cubic buildings under isothermal conditions have been intensively investigated by Hussein and Martinuzzi (1996) but few data are

available in the case of parallelepipedic buildings. One can cite the experimental work of Calluaud and David (2002) on a parallelepipedic building (18mm high with a square base of 60mm), which shape is close to the geometry of the present study. In the present simulation, the detachment distance in front of the building is 0.65 H and the re-attachment distance is 2.05 H behind it. These two values agree well with the two previously cited experimental studies that found the values of 0.38 H and 0.75 H for the detachment distance and 1.68 H and 2.70 H for the re-attachment distance.

### 3. Droplets trajectory simulation

A Lagrangian model was used to calculate the droplets trajectories. In the present simulation, the droplet mass loading, which is defined as the droplet mass per unit volume divided by the continuous-fluid mass per unit volume, is in the order of  $10^{-4}$  for a 4mm/h strong rain that is lower than the limiting value of  $10^{-3}$  (Elghobashi, 1994) so that the interaction between the carrier air and the droplets can be treated as a one-way coupling *i.e.* the droplets do not modify the wind airflow. The Lagrangian method computes the trajectory of each droplet by solving the momentum equation based on Newton's second law:

$$\frac{\pi}{6} d_d^3 \rho_d \frac{dU_i^d}{dt} = C_d \frac{\pi}{8} \rho_d^2 |U_i - U_i^d| (U_i - U_i^d) + F_e \quad (4)$$

where  $d_d$  is the droplet diameter (m),  $\rho_d$  is the droplet density ( $\text{kg/m}^3$ ),  $U_i^d$  and  $U_i$  are respectively the  $i^{\text{th}}$  component of the droplet and air instantaneous velocity (m/s),  $t$  is the time (s),  $C_d$  is the droplet drag coefficient (-) and  $F_e$  is the sum of external forces acting on the droplet (N).

In general, drag and gravity forces are the predominant forces expected in most two-phase flow systems (Loth, 2000) so that lift forces (Saffman and Magnus forces), virtual mass and stress gradient effects and Basset history term are neglected and  $F_e$  only represents the gravity and the hydrostatic pressure force in Eq. (4).

This equation is solved at each time step for every droplet. The successive locations  $x_i$  of each droplet are obtained using the following equation:

$$\frac{dx_i}{dt} = U_i^d \quad (5)$$

In order to obtain the instantaneous velocity of the fluid, its fluctuating component is calculated at each time step and for each droplet location from the turbulent characteristics of the fluid flow obtained by the air Reynolds-average calculations (previous section). Among the different models that exist in the literature, the Gosman and Ioannides (1981) model is commonly used as it compares well with experimental data in particular in the case of droplet size and can be easily coupled with CFD programs.

Thousands of droplets have been injected through a horizontal plane located at an altitude of 10m. Droplet initial horizontal velocity has been set to the undisturbed wind velocity (5m/s) while its initial vertical velocity has been calculated from the equilibrium between the gravity and the aerodynamic drag which corresponds to the terminal settling velocity of the droplet (4m/s for 1mm droplet). Droplets trajectories have been calculated until they have reached a building whole façade, the ground or a domain boundary. When a droplet hits a wall surface, it sticks to the wall at first contact and remains at this location *i.e.* no rebound, splash, run-off nor resuspension are taken into account in the present simulations.

### 4. Specific catch ratio calculation methodology

As defined by Blocken and Carmeliet (2004), the specific catch ratio ( $\eta(d_d)$ ) is calculated as the ratio of the horizontal plane ( $A_h$ ) bounded by the injection positions of the raindrops ending on the corner of the zone on the building envelope ( $A_f$ ) where the ratio has to be determined, to  $A_f$ .

$$\eta(d_d) = \frac{A_h(d_d)}{A_f} \quad (6)$$

The specific catch ratio accuracy strongly depends on the precision of the horizontal surface evaluation. A two-step procedure is employed here. Firstly, an initial guess of the horizontal surface location is obtained by simulating a few number of droplet trajectories. Secondly, a droplet injection grid is built up and the calculation of the total number of droplet (1000 droplets per grid point) trajectories is performed. Figure (3) illustrates the droplet final positions with and

without turbulence effect obtained from a rectangular horizontal injection grid constructed to cover one half of the windward façade. Without turbulence effect, the initial injection regular-spaced grid is still visible after the distortions of mean airflow whereas the added effect of the turbulence considerably modifies the droplet final location surface especially at its outlines.

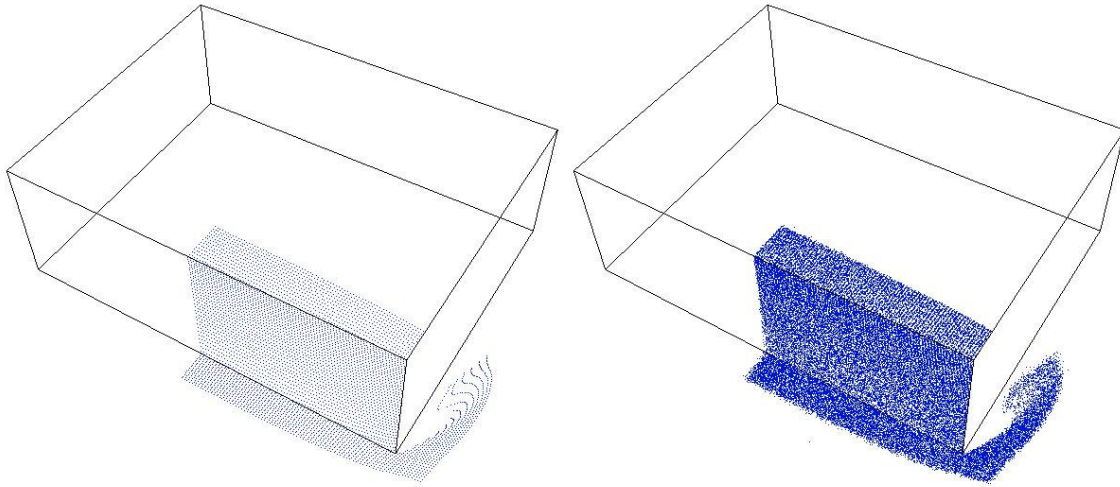


Figure 3. Droplet final locations (left: without turbulence, right: with turbulence).

## 5. Results

### 5.1. Whole windward façade

Figure (4) presents the horizontal surfaces with and without turbulence obtained from a  $5\text{cm} \times 5\text{cm}$  droplet injection grid in the case of one half of the windward façade. The colour scale represents the probability for a droplet to reach the zone on the building envelope where the ratio is to be determined. When the turbulence is neglected, the probability is 1 or 0 and the horizontal surface has a well-defined area which is close to a trapezoid but not exactly because of airflow curvatures. When the turbulence is taken into account, the probability gradually decreases on the surface edges. In this case, the surface area is calculated as the product of the grid cell area by the probability. The use of a  $5\text{cm} \times 5\text{cm}$  grid leads to a precision of  $0.23\text{m}^2$  on the whole surface area value so  $0.005$  ( $= 2\%$  of relative error) on the specific catch ratio.

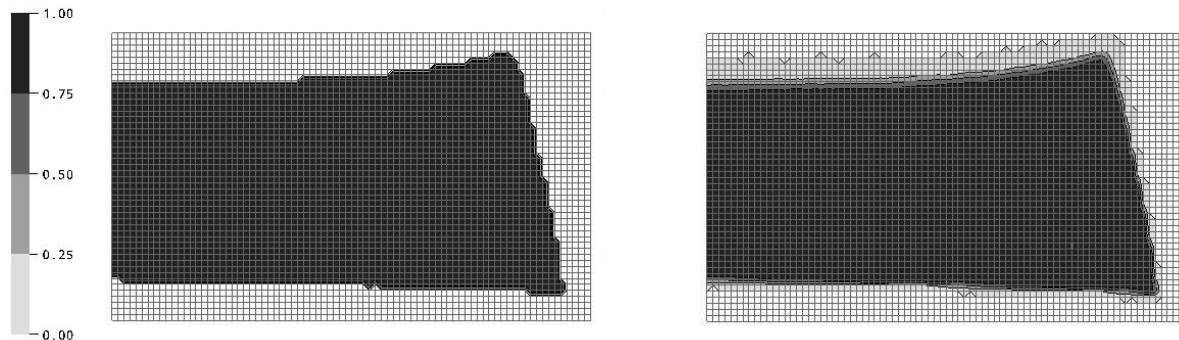


Figure 4. Horizontal surface obtained from a  $5\text{cm} \times 5\text{cm}$  droplet injection grid for one half of the whole windward façade. (left graph: without turbulence, right graph: with turbulence)

Figure (5) presents the evolution of the specific catch ratio versus the droplet number used at each grid point. Values with and without turbulence are very close ( $0.581$  and  $0.579$  respectively) so that the effect of turbulence can be neglected in the case of the whole windward surface.

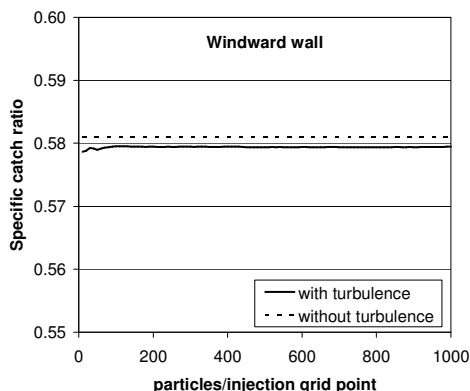


Figure 5. Specific catch ratio versus the droplet number – whole windward façade.

### 5.2. WDR gauges

It is likely to consider that the absolute effect of turbulence on the horizontal surface area would remain on the same order whatever the considered zone area on the building envelope as it depends on all the turbulence eddies encountered by the droplets and not only on the droplet final position region. Reducing the zone area where the ratio has to be evaluated can thus increase the relative effect of the turbulence. This effect can then become important for the spatial variation of the specific catch ratio of the surface that is experimentally measured using WDR gauges. As pointed out by Blocken and Carmeliet (2006), WDR gauges are of different shape and size as there is no standard to design yet. For the purpose of the present study, the droplet catchment surface area (18cm × 18cm) of the gauge developed at the Chalmers University of Technology (1999) has been chosen as a reference surface to study the variation of the specific catch ratio on the wall surface. Figure (6) presents the different locations of the wall zones where the ratio has to be determined. After first initial guesses of the droplet injection horizontal surface locations, thinner grids of 0.5cm × 0.5cm have been used to reach the precision of 0.0003m<sup>2</sup> on the surface area value so 0.005 on the specific catch ratio (= 4% of mean relative error over the different locations).

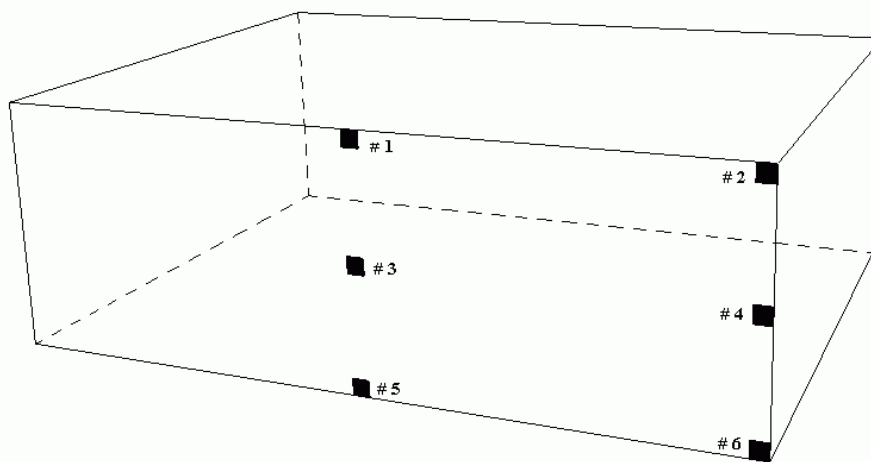


Figure 6. WDR Gauges' locations.

Figures (7) and (8) show the droplet injection horizontal surfaces associated with the droplet probability to reach the specified locations for WDR gauge #3 and #2 respectively. Concerning the first gauge, the whole horizontal surface area is increased with turbulence calculations, *e.g.*, the droplets injected in the 0.25-0.50 region have a 25 to 50% chance to reach the gauge because of turbulence, but the 0.75-1.00 region is drastically diminished presuming a reduction of the specific catch ratio. For gauge #2, as previously observed for the whole surface, the effect of turbulence lies in a small band of the surface periphery so that the specific catch ratio should not be affected considerably.

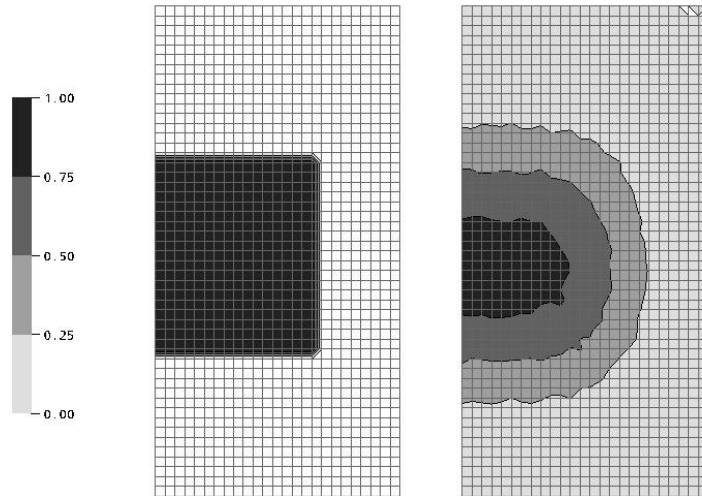


Figure 7. Horizontal surface obtained from a 5mm × 5mm droplet injection grid for WDR gauge #3. (left graph: without turbulence, right graph: with turbulence).

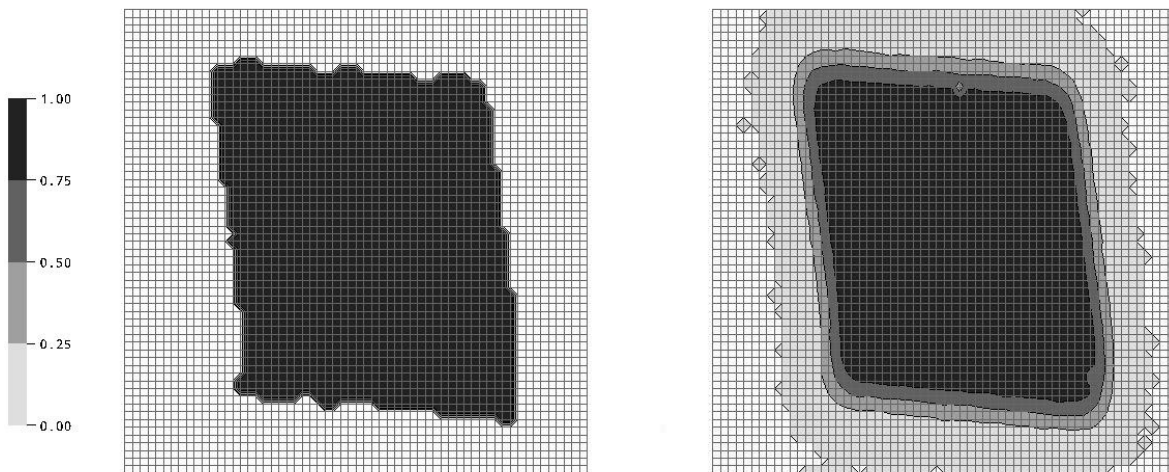


Figure 8. Horizontal surface obtained from a 5mm × 5mm droplet injection grid for WDR gauge #2. (left graph: without turbulence, right graph: with turbulence).

Figure (9) presents the evolution of the specific catch ratio versus the droplet number used at each grid point. Firstly, 200 droplets per grid point are needed to obtain a steady value of the specific catch ratio for all cases. Secondly, maximum differences between the values obtained with and without turbulence calculations are obtained for gauge #3 and #5 (5% relative difference) while there are negligible differences for gauge #2 and #4.

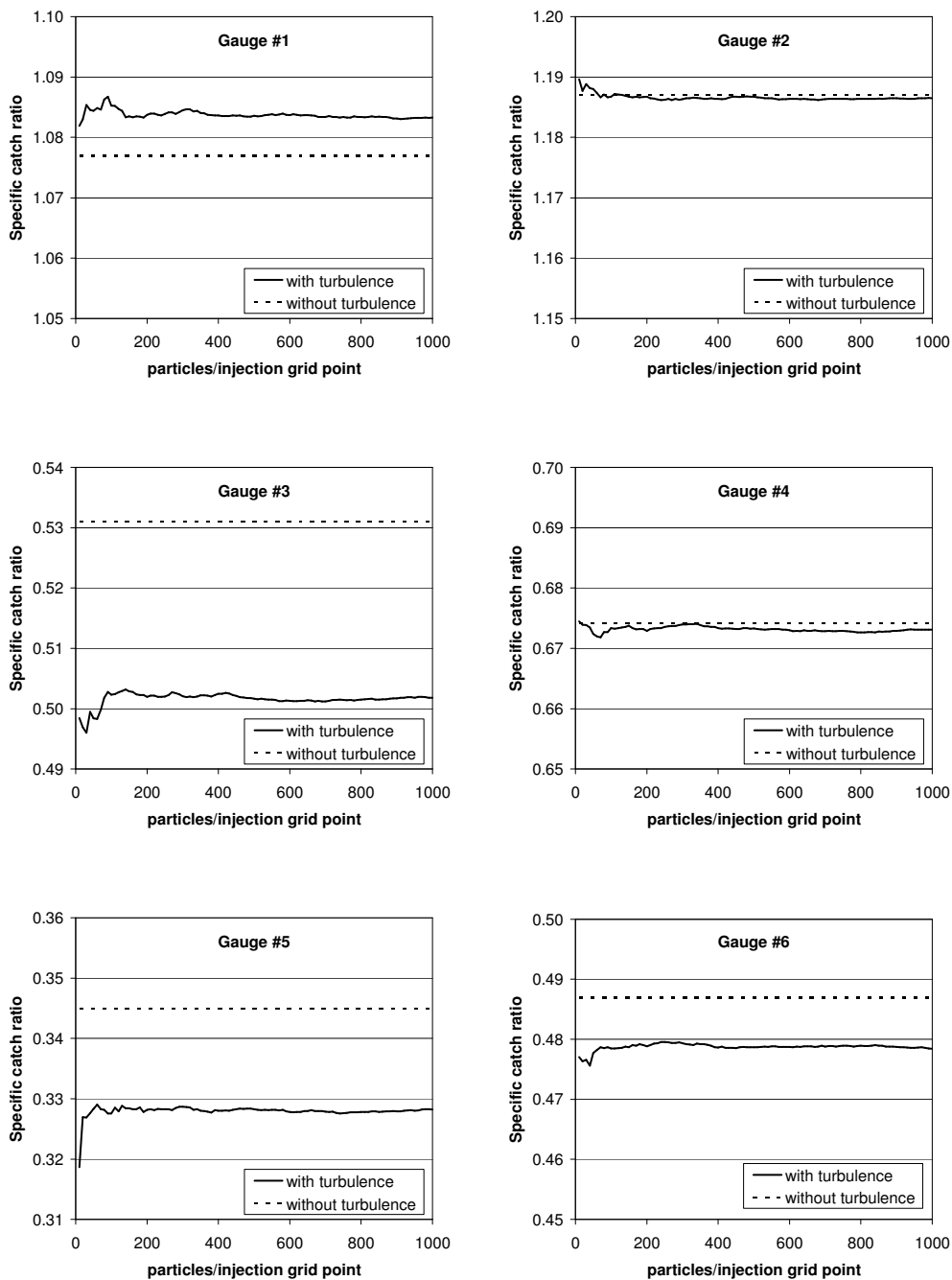


Figure 9. Specific catch ratio versus the droplet number – WDR gauges.

## 6. Discussion

Results show that turbulence on the specific catch ratio can be important in some locations in the case of WDR gauge equivalent surfaces whereas its effect is negligible in other locations or in the case of the whole windward surface. The relative importance of the airflow turbulence can be evaluated by the turbulence intensity ( $I$ ) which is calculated by dividing the airflow fluctuating velocity component ( $u'$ ), which is in the order of the turbulent kinetic energy ( $k$ ) square root in the case of isotropic turbulence, by the airflow mean velocity ( $\bar{u}$ ):

$$I = \frac{u'}{\bar{u}} \approx \sqrt{\frac{2}{3}k} \quad (7)$$

Figure (10) shows the airflow turbulence intensity obtained in the present configuration (5m/s normal wind). The isosurface represents the location where the turbulence intensity is 10%. It appears that the building is entirely contained in the region of highest turbulence intensity. In this region, the mean air velocity is so low that the relative importance of the turbulence is enhanced. A droplet trajectory has been also represented in the case of gauge #3 located in the wall centre. For the case without turbulence effect on the droplet, the trajectory is a unique undisturbed smooth curve whereas dispersion occurs all along the droplet flight when turbulence effect is considered, especially in the highest turbulence intensity zone located near the wall. As a consequence, droplets that should have reached the gauge are deviated so that the specific catch ratio is reduced.

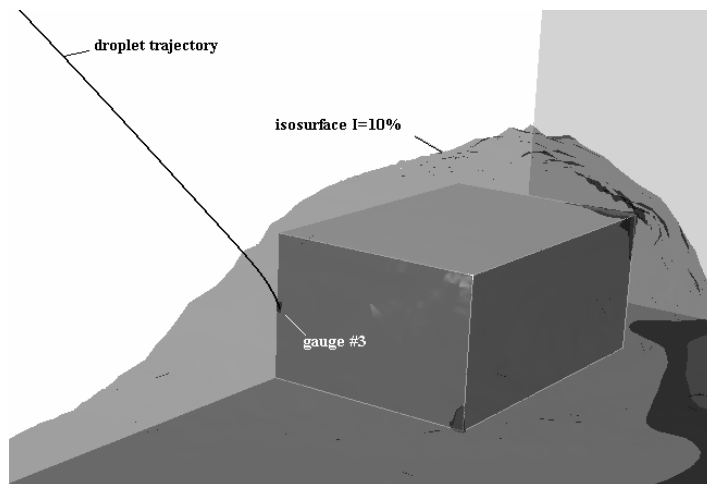


Figure 10. Turbulence intensity around the building.

Figure (11) presents the airflow turbulence intensity encountered by the droplets during their flights from their injection points to the WDR gauges. The droplet injection point has been chosen as the centre of the horizontal surface evaluated without turbulence effects. The same trend is observed for each one of the six cases. Far from the building, the droplets pass through low turbulence intensity (about 1%) regions whereas they undergo an important turbulence intensity increase while they approach the wall (at a distance lower than 3m from the wall). The increase magnitude depends on the gauge location and is clearly higher for gauges #3 and #5 which were identified as the locations where turbulence has the greater effect.

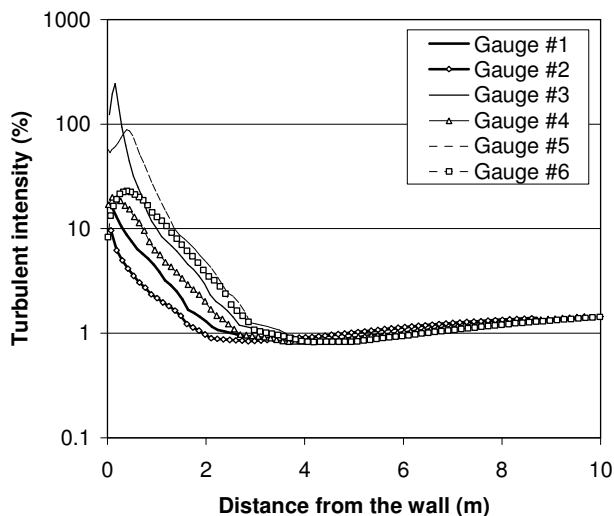


Figure 11. Turbulence intensity along droplet trajectories.

In an attempt to correlate the specific catch ratio relative error made without turbulence modelling with the turbulence intensity in the case of the WDR gauges studied here, the turbulence intensity has been integrated along the three last meters of droplet trajectory and divided by the droplet path length in order to obtain the averaged turbulence intensity value (Fig. (12)) close to the building. As expected, the relative error is an increasing function of the turbulence intensity. Best regression has been found using second-order polynomial. Considering that mean turbulence intensity commonly found around building is about 15% in unobstructed field (case of the present configuration) and 90% in urban environment at 2m high (Snyder, 1985), the relative error on the specific catch ratio would go up from 2% to 40%.

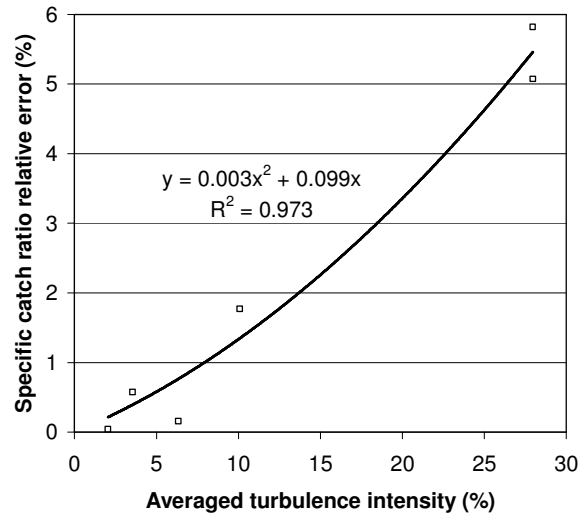


Figure 12. Specific catch ratio relative error versus airflow averaged turbulence intensity.

## 7. Conclusion

A numerical study aiming to evaluate the importance of considering turbulence on Wind-Driven Rain problems has been presented. Compared to previous studies, substantial improvements have been brought up to the airflow modelling (choice of the turbulence model and quality of the mesh grid), and the determination of the specific catch ratio (precision of the droplet injection grid and high number of injected droplets).

The present study has been limited to one droplet size, wind velocity and gauge equivalent surface area because of the prohibitive computational time induced by the calculation of millions of droplet trajectories needed to accurately evaluate the turbulence effect. Nevertheless, the following conclusions can be drawn from the present results concerning the evaluation of the WDR specific catch ratio:

- Turbulence has a negligible effect for the whole windward façade.
- In the case of smaller surfaces such as those of WDR gauges, the turbulence importance depends on the location of the considered surface. Maximal relative error of 5% induced by neglecting turbulence has been found for a gauge located at the wall surface centre.
- 200 is the minimum number of droplets to be injected per horizontal surface grid point to accurately calculate the specific catch ratio.
- Close examination of the airflow turbulence intensity provides useful information to evaluate the error induced by neglecting the turbulence effect.

The main conclusion of the present study is that turbulence can be neglected for similar WDR problems *i.e.* same droplet sizes (and coarser ones) and wind velocities, simple building shapes and isolated buildings. However, turbulence effect can be considerably enhanced for irregular shape buildings, real three-dimensional gauges and even more in the case of the presence of other buildings in the surrounding. For this last case, turbulence calculations would then be needed to correctly evaluate the WDR on building façades as we have shown that relative errors can be as high as 40%.

## 8. Acknowledgements

The authors thank the Brazilian Research Council (CNPq) of the Secretary for Science and Technology of Brazil for support of this work.

## 9. References

- Best, A.C., 1950, "The size distribution of raindrops", *Quart. J. of the Royal Meteor. Soc.*, Vol. 76, pp. 16–36.
- Blocken, B. and Carmeliet, J., 2002, "Spatial and temporal distribution of driving rain on a low-rise building", *Wind and Struct.*, Vol. 5, pp. 441–462.
- Blocken, B. and Carmeliet, J., 2004, "A review of wind-driven rain research in building science", *J. Wind Eng. Ind. Aerodyn.*, Vol. 92, pp. 1079–130.
- Blocken, B. and Carmeliet, J., 2006, "On the accuracy of wind-driven rain measurements on buildings", *Building and Env.* In-Press, corrected proof.
- Calluau, D. and David, L., 2002, "Backward projection algorithm and stereoscopic particle image velocimetry measurements of the flow around a square section cylinder", 11<sup>th</sup> Int. Symp. Applications of Laser Techn. to Fluid Mech.
- CFX, 2004, CFX-5 Solver Theory.
- Choi, E.C.C., 1997, "Numerical modelling of gust effect on wind-driven rain", *J. of Wind Eng. Ind. Aerodyn.*, Vol. 72, pp. 107–116.
- Choi, E.C.C., 1999, "Wind-driven rain on building faces and the driving-rain index", *J. of Wind Eng. Ind. Aerodyn.*, Vol. 79, pp. 105–122.
- Davenport, A.G., "Rationale for Determining Design Wind Velocities", *Journal of the Structural Division, Proceedings American Society Civil Engineers*, Vol. 86, pp. 39–68.
- Elghobashi, S., 1994, "On predicting particle-laden turbulent flows", *Appl. Scient. Research*, Vol. 52, pp. 309–329.
- Fothergill, C.E., Roberts, P.T. and Packwood, A.R., 2002, "Flow and dispersion around storage tanks. A comparison between numerical and wind tunnel simulations", *Wind and Struct.*, Vol. 5 2-4, pp. 89–100.
- Gosman, A.D. and Ioannides, E., 1981, "Aspects of computer simulation of liquid-fuel combustor". AIAA 19<sup>th</sup> Aerospace Science Meeting, St Louis, paper 81–0323.
- Hagan, H., 1999, "Wind-driven rain studies. A C-FD-E approach", *J. of Wind Eng. Ind. Aerodyn.*, Vol. 81, pp. 323–331.
- Högberg, A.B., Kragh, M.K. and van Mook, F.J.R., 1999, "A comparison of driving rain measurements with different gauges", *Proc. of the 5<sup>th</sup> symp. of building physics in the Nordic Countries*, Gothenburg, pp. 361–368.
- Hussein, H.J. and Martinuzzi, R.J., 1996, "Energy balance for turbulent flow around a surface mounted cube placed in a channel", *Physics of Fluids*, Vol. 8, pp. 764–780.
- International Energy Agency, 2006, "Annex 41, Whole building heat, air and moisture response (MOIST-EN)", <http://www.kuleuven.ac.be/bwf/projects/annex41/index.htm>.
- Karagiozis, A., Hadjisophocleous, G. and Cao, S., 1997, "Wind-driven rain distributions on two buildings", *J. of Wind Eng. Ind. Aerodyn.*, Vol. 67–68, pp. 559–72.
- Künzel, H.M., 1994, "Simultaneous heat and moisture transport in building components: one- and two-dimensional calculation using simple parameters", PhD dissertation, University of Stuttgart.
- Judkoff, R.D. and Neymark, J.S., 1995, "Building Energy Simulation Test (BESTEST) and Diagnostic Method", NREL/TP-472-6231, Golden, Colorado National renewable Energy Laboratory.
- Lakehal, D., Mestayer, P.G., Edson, J.B., Anquetin, S. and Sini, J.-F., 1995, "Eulero-lagrangian simulation of raindrop trajectories and impacts within the urban canopy", *Atm. Env.*, Vol. 29, pp. 3501–3517.
- Loth, E., 2000, "Numerical approaches for motion of dispersed particles, droplets and bubbles", *Progress in Energy Comb. Sc.*, Vol. 26, pp. 161–223.
- Mendes, N., Oliveira, R.C.L.F. and dos Santos, G.H., 2003, "DOMUS 2.0: A whole-building hygrothermal simulation program", 8<sup>th</sup> Int. IBPSA Conf., Eindhoven, Netherlands.
- Menter, F.R., 1993, "Multiscale model for turbulent flows", Int. 24<sup>th</sup> Fluid Dyn. Conf., American Inst. Aeron. Astron.
- Meroney, R.N., Leidl, B.M., Rafailidis, S. and Schatzmann, M., "Wind-tunnel and numerical modeling of flow and dispersion about several building shapes", *J. of Wind Eng. Ind. Aerodyn.*, Vol. 81, pp. 333–345.
- Sankaran, R. and Paterson, D.A., 1995, "Computation of rain falling on a tall rectangular building", 9<sup>th</sup> Int. Conf. on Wind Eng., New Delhi, India, pp. 2127–2137.
- Sedlbauer, K., 2001, "Vorhersage von schimmelpilzbildung auf und in bauteilen", PhD dissertation, University of Stuttgart.
- Snyder, W.H., 1985, "Fluid modeling of pollutant transport and diffusion in stably stratified flows over complex terrain", *Ann. Rev. Fluid Mech.*, Vol. 17, pp. 239–266.
- Van Mook, F.J.R., de Wit, M.H. and Wisse, J.A., 1997, "Computer simulation of driving rain on buildings envelopes", 2<sup>nd</sup> European and African Conf. on Wind Eng., 22–26 June.

## 10. Copyright Notice

The author is the only responsible for the printed material included in his paper.